

Peculiar ferromagnetic insulator state in the low-hole-doped manganites

P. A. Algarabel,* J. M. De Teresa, J. Blasco, and M. R. Ibarra

Departamento de Física de la Materia Condensada and Instituto de Ciencia de Materiales de Aragón, Universidad de Zaragoza and Consejo Superior de Investigaciones Científicas, 50009 Zaragoza, Spain

Cz. Kapusta, M. Sikora, and D. Zajac

Department of Solid State Physics, Faculty of Physics and Nuclear Techniques, University of Mining and Metallurgy, 30-059 Cracow, Poland

P. C. Riedi

Department of Physics and Astronomy, University of St. Andrews, Fife, KY169SS, Scotland, United Kingdom

C. Ritter

Institute Laue Langevin, Boite Postale 156, 38042 Grenoble Cedex, France

(Received 23 October 2002; published 3 April 2003)

In this work we show the very different nature of the ferromagnetic state of the low-hole-doped manganites with respect to other manganites showing colossal magnetoresistance. High-field measurements definitively prove the coexistence of ferromagnetic-metallic and ferromagnetic-insulating regions even when the sample is magnetically saturated, with the ground state being inhomogeneous. We have investigated $\text{La}_{0.9}\text{Ca}_{0.1}\text{MnO}_3$ as a prototype compound. A wide characterization by means of magnetic and magnetotransport measurements, neutron diffraction, small-angle neutron scattering, and nuclear magnetic resonance has allowed us to establish that the ground state is based on the existence of disordered nanometric double-exchange metallic clusters that coexist with long-range superexchange-based ferromagnetic insulating regions. Under high magnetic field the system reaches magnetization saturation by aligning the magnetic clusters and the insulating matrix, but even if they grow in size, they do not reach the percolation limit.

DOI: 10.1103/PhysRevB.67.134402

PACS number(s): 76.60.-k, 61.12.Ex, 75.25.+z

I. INTRODUCTION

Much effort has been expended during recent years to understand the great variety of phenomena found in manganites (see as review examples Refs. 1–3). The existence of mixed valences in these compounds either by cation substitution or oxygen nonstoichiometry in the strongly correlated (high spin configuration) and Jahn-Teller insulating LaMnO_3 gives rise to the existence of Mn^{+4} ions. As a consequence, itinerant holes of e_g symmetry are present and can hop by lowering their kinetic energy and broadening the e_g bands when core t_{2g} effective spins are parallel. This is the basis of the double-exchange interaction that is responsible for the coexistence of the long-range ferromagnetic order and metallic state. In fact, the field effect on the transition from paramagnetic-insulator to ferromagnetic-metallic state produces colossal magnetoresistance (CMR) discovered by Jin *et al.*⁴ in the compound $\text{La}_{0.6}\text{Y}_{0.07}\text{Ca}_{0.33}\text{MnO}_3$. This finding triggered interest in these fascinating compounds. Early evidence for nanoscopic phase segregation was found above the Curie temperature in the above-mentioned compound.^{5,6} Phase segregation tuned by the Mn-O-Mn bond angle (i.e., the electron bandwidth) was proposed in the $(\text{La}_{1-x}\text{Tb}_x)_{2/3}\text{Ca}_{1/3}\text{MnO}_3$ series⁷ and by O^{18} isotopic exchange in the compound $(\text{La}_{0.5}\text{Nd}_{0.5})_{2/3}\text{Ca}_{1/3}\text{MnO}_3$.⁸ The assumption of the coexistence of metallic low-volume and insulating large-volume regions was definitively proved by dark image electron microscopy.⁹ All the observed phenomena were explained on the basis of ferromagnetic double ex-

change, antiferromagnetic superexchange interaction, and charge and orbital ordering. The low-hole-doping region ($x < 0.125$) of the $\text{La}_{1-x}\text{Ca}_x\text{MnO}_3$ series^{10,11} as well as the oxygen-deficient $\text{LaMnO}_{3-\delta}$ (Ref. 12) compounds showed the existence of superexchange ferromagnetic-insulating states and the existence of metallic short-range ferromagnetic clusters (10–40 Å). A pioneering neutron-diffraction experiment already pointed to the existence of ferroantiferromagnetic coexisting regions.¹³ Recent small-angle neutron scattering (SANS),¹² inelastic neutron scattering,¹¹ as well as nuclear-magnetic-resonance (NMR) experiments^{10,14} provided insight based on the existence of metallic clusters with short-range ferromagnetic order and the existence of two magnon dispersion branches associated with double-exchange and superexchange ferromagnetic interactions, respectively. It is difficult to provide a unified picture in this concentration region given the subtle energy balance arising from the interplay between the above-mentioned competing interactions. In this paper we will concentrate on the $\text{La}_{0.9}\text{Ca}_{0.1}\text{MnO}_3$ compound, in which a ferromagnetic-insulating state was found. The lack of microscopic characterization of this compound under high magnetic field leads to some misunderstanding on the ground state in this prototype compound. We give an extensive characterization by using magnetic and magnetotransport macroscopic probes as well as NMR under high magnetic field, neutron diffraction, and SANS under high magnetic field. This has allowed us to give a comprehensive description of the low-temperature ground state in which, even at satura-

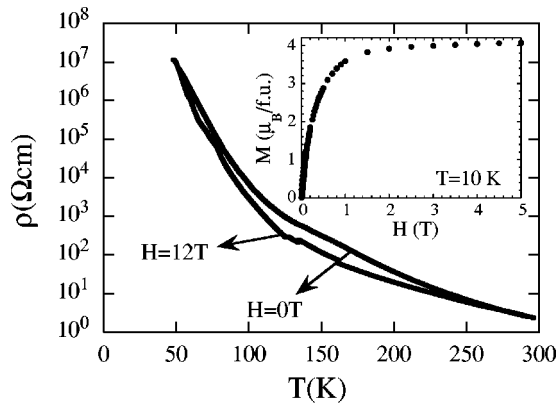


FIG. 1. Thermal dependence of the resistivity at zero field and under the maximum available field (12 T) of $\text{La}_{0.9}\text{Ca}_{0.1}\text{MnO}_3$. The inset shows the magnetization isotherm at 10 K.

tion, insulating superexchange ferromagnetic regions coexist with nonpercolating metallic double-exchange ferromagnetic regions.

II. EXPERIMENT

The sample was prepared by a standard ceramic procedure. Stoichiometric proportions of La_2O_3 , CaCO_3 , and MnCO_3 with nominal purities not less than 99.99% were mixed and heated in air at 950°C for 12 h. After grinding, the powder was pressed into bars and sintered in air at 1250°C for 48 h and 1400°C for 12 h with intermediate grinding. The oxygen content was analyzed using standard redox titration with KMnO_4 and Mohr's salt. A step-scanned powder-diffraction pattern using a D-Max Rigaku system with rotating anodes confirmed the quality of the sample used in our experiments. Magnetic measurements were performed using a superconducting quantum interference device magnetometer. The resistivity measurements were performed by using the four-points technique and the high-field measurement using a 12-T superconducting coil. Neutron-diffraction experiments were performed on two different instruments at the high-flux reactor in the Institute Laue-Langevin. (ILL) D1B ($\lambda = 2.52 \text{ \AA}$) and high-resolution D2B ($\lambda = 1.594 \text{ \AA}$) instruments were used to refine the crystal parameters and the magnetic structure at several temperatures. The SANS experiments were performed with the instrument D16 using a wavelength of 4.5 \AA and a resolution in the transfer momentum vector Q of $5 \times 10^{-3} \text{ \AA}^{-1}$, within the range $0.03 < Q < 0.65 \text{ \AA}^{-1}$. For NMR measurements, an automated frequency swept spin-echo spectrometer was used within a broad range of temperatures and fields up to 6 T. Spin-echo spectra were obtained by measuring the integrated echo intensity vs frequency, ν . In addition, a two-pulse sequence with the amplitude/length of the pulses adjusted to a maximum echo signal for a given spectrum was used.

III. MACROSCOPIC BEHAVIOR

The resistivity measurements shown in Fig. 1 indicate the insulating nature of this system even in the low-temperature range where the system is ferromagnetically long-range or-

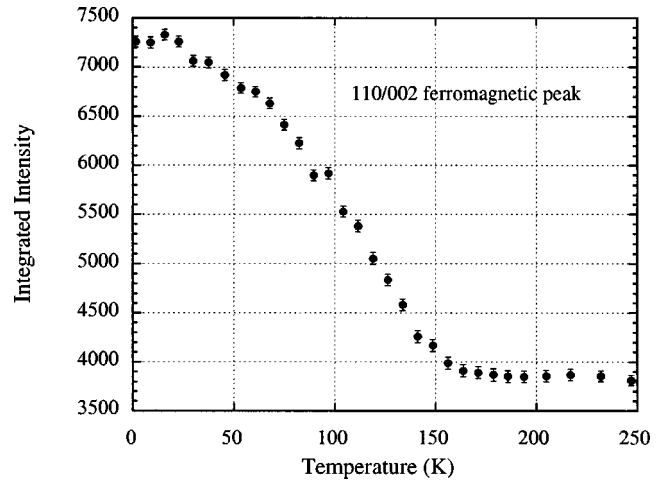


FIG. 2. Thermal dependence of the integrated intensity of the (110/002) Bragg peak of $\text{La}_{0.9}\text{Ca}_{0.1}\text{MnO}_3$ obtained on a D1B instrument at ILL.

dered ($T_C = 160 \text{ K}$). This situation persists at the largest available steady magnetic field of 12 T. In the inset of Fig. 1 we show the magnetization isotherm at low temperature ($T = 10 \text{ K}$) in which magnetic saturation is achieved at applied magnetic fields larger than 2 T, quite a large field if we consider the low magnetic anisotropy of the ferromagnetic manganites. The existence of noninteracting ferromagnetic clusters embedded in an insulating ferromagnetic matrix, as we explain later, could explain the shape of these magnetization results. Due to the small size of the ferromagnetic clusters, typically 3 nm, one can expect a very low blocking temperature. In fact we did not observe any anomaly in the low-field dc magnetic-susceptibility measurements down to 4 K associated with this effect. Then, one can expect a superparamagnetic behavior of the magnetic clusters. We explain the large magnetic susceptibility at low field ($< 1 \text{ T}$) as originating from the domain-wall movement under field in the matrix, and the high-field susceptibility ($> 1 \text{ T}$) as due to the orientation of the clusters along the magnetic field against the thermal energy. This picture, as we argue in the next sections, would be consistent with a spontaneous magnetization of $3.2\mu_B$ due to the ferromagnetic-insulating matrix and a field-induced magnetization originating in the rotation of the magnetic clusters, reaching the saturation value of $3.9\mu_B$ at 3 T. The hypothesis of a percolation of the double-exchange clusters at the larger fields is ruled out because of the absence of metallic behavior even at 12 T.

IV. NEUTRON DIFFRACTION AND SANS

Spontaneous magnetization was unambiguously obtained from the refinement of the neutron-diffraction experiments on D1B and D2B. The thermal dependence of the integrated intensity of the [110/002] nuclear Bragg peak is shown in Fig. 2. This is a clear signature of the existence of long-range ferromagnetic order below $T_C = 160 \text{ K}$. In Fig. 3 we present the refined pattern obtained on D2B at $T = 1.5 \text{ K}$ for our $\text{La}_{0.9}\text{Ca}_{0.1}\text{MnO}_3$ sample. Although a mixture of ferromagnetic and A-type antiferromagnetic regions have been pro-

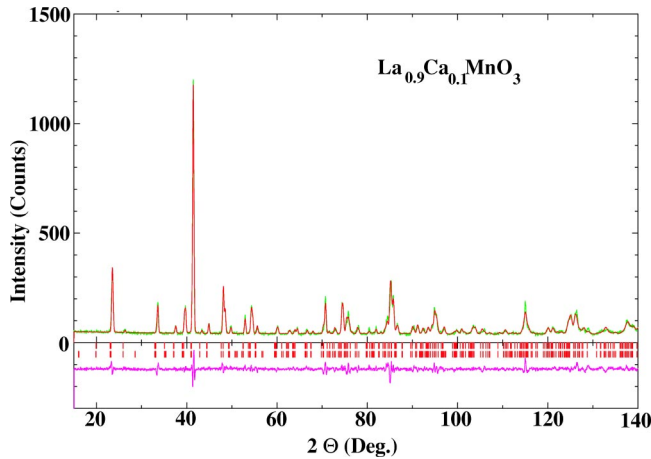


FIG. 3. Neutron-diffraction intensity and refined pattern of $\text{La}_{0.9}\text{Ca}_{0.1}\text{MnO}_3$ obtained at $T = 1.5$ K on a D2B instrument at ILL.

posed in low-hole-doped manganites,¹³ we find no evidence of antiferromagnetic domains in our sample. However, in another sample with a nominally close composition, $\text{La}_{0.875}\text{Ca}_{0.125}\text{MnO}_3$, around 10% of the A-type antiferromagnetic phase has been detected.¹⁵

Using the hypothesis of a monophasic system, the refined ferromagnetic moment of our sample amounts to only $3.3\mu_B$. If on the contrary the possibility of a phase segregation is admitted, and assuming a theoretical moment of $3.9\mu_B$ per Mn (with the presence of 10% Mn^{4+} ions), around 30% of the Mn spins must not be long-range ordered.

In this context the existence of a significant contribution to the SANS intensity below $T_C = 160$ K constitutes a clear hallmark of the existence of short-range ferromagnetic regions. In Fig. 4, a comparison between the thermal dependence of the SANS intensity in $\text{La}_{0.9}\text{Ca}_{0.1}\text{MnO}_3$ and $\text{La}_{0.6}\text{Y}_{0.07}\text{Ca}_{0.33}\text{MnO}_3$ is shown. In the case of $\text{La}_{0.6}\text{Y}_{0.07}\text{Ca}_{0.33}\text{MnO}_3$, the magnetic SANS intensity appears in the paramagnetic state, which was associated with nanometric short-range double-exchange clusters.¹⁶ On the other hand, for $\text{La}_{0.9}\text{Ca}_{0.1}\text{MnO}_3$ the magnetic SANS intensity appears in the ferromagnetic state.

From the fit of the q dependence of the intensity of the

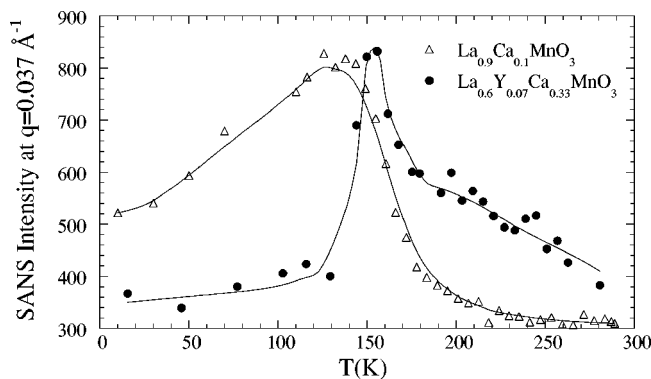


FIG. 4. Thermal dependence of the SANS intensity. For the sake of clarity, a comparison with the results on $\text{La}_{0.6}\text{Y}_{0.07}\text{Ca}_{0.33}\text{MnO}_3$ is shown (Ref. 16). Lines are visual guides.

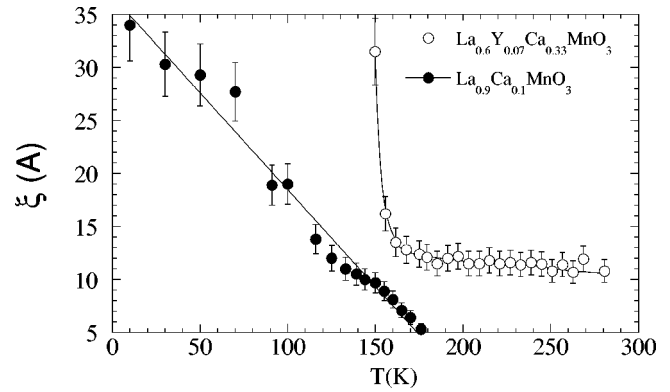


FIG. 5. Thermal dependence of the magnetic correlation length, ξ . For the sake of clarity a comparison with the results on $\text{La}_{0.6}\text{Y}_{0.07}\text{Ca}_{0.33}\text{MnO}_3$ is shown (Ref. 16). Lines are visual guides.

SANS contribution using squared-Lorentzian functions $\{I = I_0/[q^2 + (1/\xi)^2]^2\}$, we have obtained the magnetic correlation length, ξ , which is associated with the size of the magnetic clusters. The squared-Lorentzian behavior in the SANS intensity is expected for static cluster scattering.¹⁷ In Fig. 5 we show the thermal dependence of ξ and we can observe the appearance of the clusters below 170 K, which is close to the setting temperature for long-range ferromagnetic order. The clusters increase in size as the temperature decreases, reaching the value of 3–3.5 nm at low temperatures. We would like to emphasize that this behavior is completely different from that found in the optimized CMR concentration region ($x = 0.33$). In the latter case there exists 1–3-nm ferromagnetic clusters in the paramagnetic phase and, as the long-range-order temperature (insulator-metal transition temperature) is approached from above, ξ sharply increases and the SANS contribution disappears around T_C . For the sake of clarity and comparison we have included our previous results on $\text{La}_{0.6}\text{Y}_{0.07}\text{Ca}_{0.33}\text{MnO}_3$ in Fig. 5. Clearly, from these results we can see the very different nature of the ferromagnetic phase in both compounds. In the case of $x = 0.33$ the ferromagnetic phase is homogeneous and metallic due to the double-exchange interaction, unlike the reported $x = 0.1$ compound in which the ferromagnetic clusters still persist at low temperature in a fraction of about 30%.

V. NMR UNDER HIGH FIELD

We can get insight into the nature of the low-temperature phase by performing NMR experiments under high magnetic field. The very relevant information that we can obtain from these experiments is, first, whether the short-range correlation within the clusters is of a double-exchange origin (electron hopping $\text{Mn}^{3+}\text{-Mn}^{4+}$, and consequently metallic) and second, whether these metallic clusters persist even under an applied magnetic field.

A zero-field ^{55}Mn NMR study of the compound has recently been presented in Ref. 10. The resonant lines have been identified and attributed to charge localized Mn^{4+} and Mn^{3+} states that are present in the ferromagnetic-insulating (FI) matrix as well as to the delocalized double-exchange (DE) states corresponding to the ferromagnetic clusters. The

line assignment was based on the resonant frequency characteristics of these states and on their temperature dependencies. Namely, the DE line showed the same temperature dependence as the resonant line of the double-exchange ferromagnetic compound $\text{La}_{0.67}\text{Ca}_{0.33}\text{MnO}_3$, whereas the resonant frequency of the charge localized state revealed a much faster decrease with increasing temperature (see Fig. 3 of Ref. 10). This provided an unambiguous identification for the DE line and was proof of the presence of DE clusters in the $\text{La}_{0.9}\text{Ca}_{0.1}\text{MnO}_3$ compound. In order to determine the relative amount of the FI phase and for a comparison to the SANS results, the study of the ^{55}Mn NMR spin-echo spectra in the applied magnetic field, at various temperatures and excitation conditions, has been carried out. Also, the ^{139}La spectrum has been measured.

The ^{55}Mn and ^{139}La signals at zero field exhibit an NMR enhancement factor an order-of-magnitude smaller than those in $\text{La}_{0.67}\text{Ca}_{0.33}\text{MnO}_3$, where a typical domain-wall enhancement is observed. The enhancement decreases by a factor less than 2 upon application of 1-T external field, whereas in $\text{La}_{0.67}\text{Ca}_{0.33}\text{MnO}_3$ it decreases by an order of magnitude. Since such a field usually removes domain walls, the NMR signal of the compound can be attributed mostly to magnetic domains. The spectrum at 4.2 K and zero field has been decomposed into a set of Gaussian lines centered at 318 (Mn^{4+}), 380 (DE), and four peaks at 407–525 MHz (Mn^{3+}). The NMR enhancement of the DE and Mn^{3+} peaks is similar to and for Mn^{4+} slightly larger than the other peaks.

In order to eliminate the remanent domain-wall signal and obtain better-resolved resonance lines, the spectra at 4.2 K and zero field have also been measured at larger pulse separations, so that the signals originating from domain walls could relax out due to a faster spin-spin relaxation. The DE peak does not show a noticeable minimum of the spin-spin relaxation time at its center, which indicates that the DE clusters are of nanometer size.¹⁸ In metallic ferromagnetic compounds such as $\text{La}_{0.67}\text{Ca}_{0.33}\text{MnO}_3$ it shows a much shorter spin-spin relaxation time (T_2) at the line center caused by the Suhl-Nakamura relaxation due to coupling of nuclear spins by virtual magnons.¹⁹ This interaction has a range of 3.5 nm in these compounds at low temperatures,¹⁸ and is not effective in nanometer-size clusters where only a few Mn ions inside clusters, which contribute to the center of the NMR line, have the same magnetic environment. The DE line also shows a linewidth about two times larger than that in the $\text{La}_{0.67}\text{Ca}_{0.33}\text{MnO}_3$ compound, which may be related to a much lower DE hopping rate than in $\text{La}_{0.67}\text{Ca}_{0.33}\text{MnO}_3$.

Another proof of a two-phase character of the ground state of the compound comes from the ^{139}La spectrum (see Fig. 6). It consists of two resonance lines located at 15 and 32 MHz of the same NMR enhancement. A similar two-line pattern has been observed in the ^{139}La spectra of $\text{La}_{0.875}\text{Sr}_{0.125}\text{MnO}_3$ and $\text{La}_{0.85}\text{Sr}_{0.15}\text{MnO}_3$.²⁰ Since the more insulating $\text{La}_{0.875}\text{Sr}_{0.125}\text{MnO}_3$ compound exhibits a larger intensity of the upper line, this line can be attributed to FI regions also in $\text{La}_{0.9}\text{Ca}_{0.1}\text{MnO}_3$. Thus, the lower line is assigned to the DE clusters. However, its resonant frequency, 15 MHz, is nearly 30% lower than that of the 21 MHz in

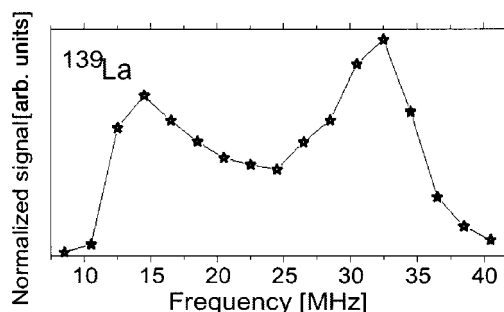


FIG. 6. ^{139}La spin-echo spectrum at 4.2 K of $\text{La}_{0.9}\text{Ca}_{0.1}\text{MnO}_3$. The line is a visual guide.

metallic $\text{La}_{0.67}\text{Ca}_{0.33}\text{MnO}_3$, which indicates that the DE regions differ from those in $\text{La}_{0.67}\text{Ca}_{0.33}\text{MnO}_3$ and can imply that the DE interaction is less effective here than in $\text{La}_{0.67}\text{Ca}_{0.33}\text{MnO}_3$. A single resonance line of ^{139}La has recently been reported in Ref. 21. In fact, at low pulse power a single line is observed corresponding to a large enhancement factor.

The analysis of the temperature dependence of the spectra shows that with increasing temperature the Mn^{3+} lines decrease in intensity faster than do the DE and Mn^{4+} lines (see Fig. 7). This is due to a faster increase of the spin-spin relaxation rate with temperature for the Mn^{3+} lines. The Mn^{4+} line exhibits approximately two times longer T_2 at the whole temperature range, disappearing at about 77 K. This can be attributed to a melting of charge localized states possibly due to the excitation of small Jahn-Teller polarons as postulated recently in Ref. 14.

In order to study the evolution of charge localized phase and DE clusters in the magnetic field, ^{55}Mn spin-echo spectra have been measured under several selected applied magnetic fields (see Fig. 8). The pulse power/length has been adjusted for the individual spectra to the maximum signal. A shift of the resonance lines towards lower frequencies with increasing applied field is observed. This is due to a partial cancellation of the hyperfine field which is mostly of a core electron polarization origin and is antiparallel to the Mn spin moments aligning with the field. The Mn^{4+} line shows a shift consistent with a full ^{55}Mn gyromagnetic ratio, which indicates a parallel alignment of the Mn^{4+} moments with the field. The DE peak shows a smaller shift up to 3 T that can possibly be related to a noncolinear alignment of the moments of DE clusters in such a field. However, between 3 and 6 T, the shift also corresponds to a full gyromagnetic ratio, i.e., to a parallel alignment of the moments of DE clusters with the field at such fields.

In order to determine an approximate amount of the DE clusters, the spectra at the applied field have been fitted with sets of Gaussian lines and the areas have been corrected for the NMR enhancement. The values obtained can be regarded as measures of the amount of the corresponding Mn states and, consequently, the amount of FI and the DE controlled phases. Since the DE peak (380 MHz at zero field) was not clearly resolved from an order-of-magnitude smaller Mn^{3+} line (407 MHz at zero field) at the applied field, they were fitted together with one Gaussian line. In order to determine

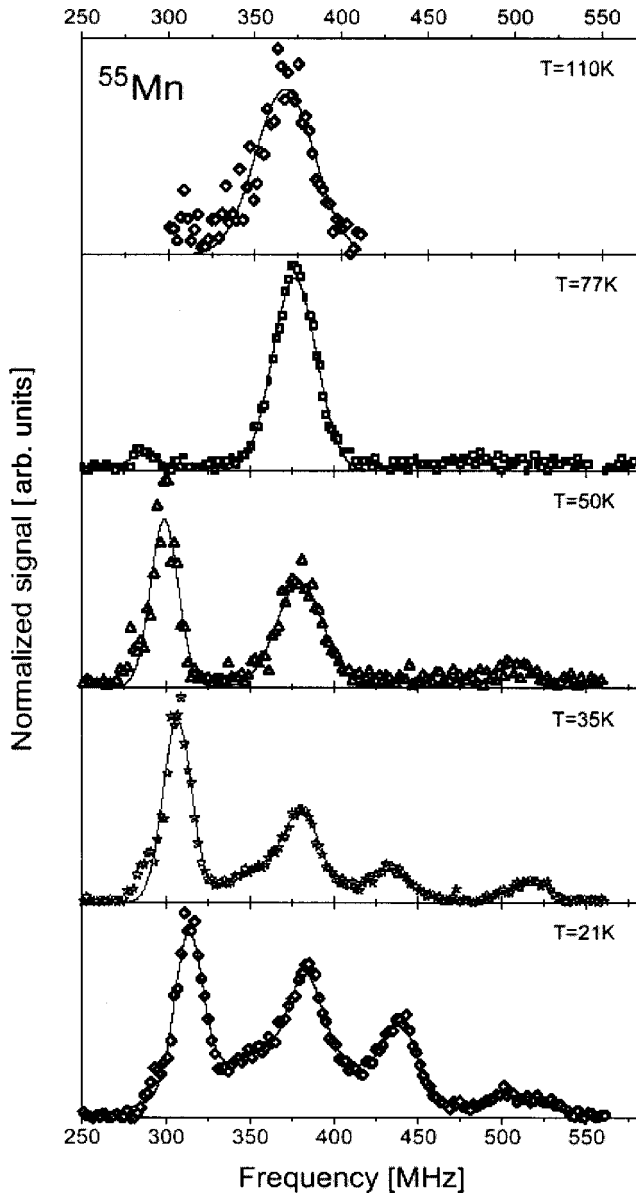


FIG. 7. ^{55}Mn spin-echo spectra of $\text{La}_{0.9}\text{Ca}_{0.1}\text{MnO}_3$ at various temperatures. Solid lines represent fits with sets of Gaussian lines (see text).

the amount of the DE clusters at various fields the corrected area of the DE line has been compared to the corrected areas of all lines within individual spectra. The corresponding amount of the DE phase with respect to the insulating ferromagnetic phase was estimated to be $(42 \pm 5)\%$ at 0 T. It grows to $(66 \pm 10)\%$ at 6 T, which is possibly related to a growth of the DE clusters with the applied field.

It is worth noting that a very similar pattern of 4+ DE and 3+ lines to that in $\text{La}_{0.9}\text{Ca}_{0.1}\text{MnO}_3$ is obtained in other compounds, e.g., $\text{La}_{0.875}\text{Ca}_{0.125}\text{MnO}_3$ or $\text{LaMnO}_{3+\delta}$.^{10,20,22} Relative intensities of the lines are similar and do not follow the ratio of Mn^{4+} to Mn^{3+} , which can be deduced from the doping level. A possible explanation for the effect is that the interior of the superexchange controlled FI phase exhibits a very fast nuclear relaxation preventing observation of the NMR spin-echo signal from these regions, where the nomi-

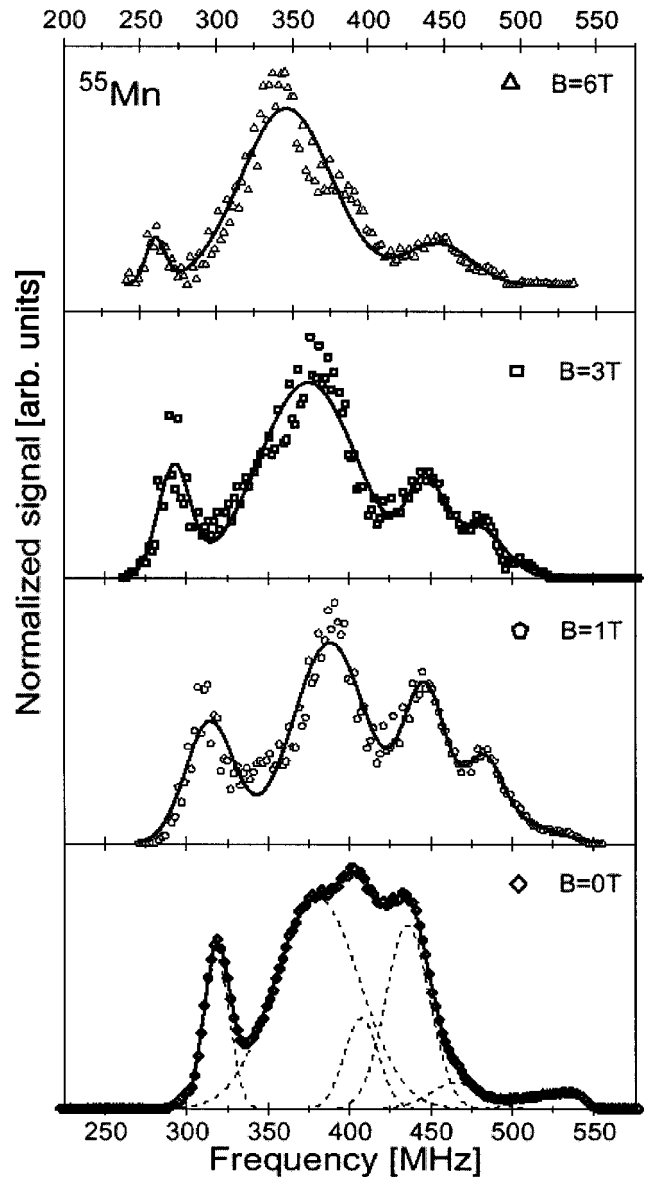


FIG. 8. ^{55}Mn spin-echo spectra of $\text{La}_{0.9}\text{Ca}_{0.1}\text{MnO}_3$ at 3 K and various applied magnetic fields. Solid lines represent fits with sets of Gaussian lines (see text).

nal Mn^{4+} to Mn^{3+} ratios should be observed. Such a wipe-out of the ^{139}La NMR signal was reported for several hole-doped insulating compounds in Refs. 14 and 21 and attributed to the lattice excitations identified as small Jahn-Teller polarons. Thus, the NMR signal observed originates from the DE clusters and FI states at their boundaries, so that it reflects the amount of DE phase with respect to the FI states within the cluster plus boundary regions, not in the whole sample. As a consequence, the amount of the DE phase with respect to the FI phase determined from the NMR spectra is possibly overestimated.

VI. CONCLUSIONS

The wide macro- and microscopic characterization of the compound $\text{La}_{0.9}\text{Ca}_{0.1}\text{MnO}_3$ has allowed us to definitively es-

establish the nonhomogeneous nature of the ferromagnetic insulating state in the low-doping hole region of La-Ca mixed-valence manganites. Neutron diffraction shows the fraction of disordered manganese spins to be close to 30%. On the other hand SANS results reveal the existence of nanometric ferromagnetic clusters (3–4 nm). The major ferromagnetic phase is insulating and consequently, the ferromagnetic superexchange mechanism should prevail, with the short-range DE interaction responsible for the formation of the ferromagnetic clusters. Then, one can determine a ground state in which disordered ferromagnetic clusters are embedded in an insulating ferromagnetic background. This situation is compatible with the existence of two different branches found in the magnon dispersion curves.¹¹ NMR results pointed to the coexistence of DE and superexchange regions clearly associated with the presence of well-defined resonance lines at characteristic frequencies. The metallic nature of the clusters was inferred from the analysis of the NMR spectra. NMR under field reveals the presence of DE and superexchange lines even at saturation. The applied magnetic field increases the size of the DE clusters but percolation is not achieved.

This is an exciting result in the phenomenology of manganites: from the magnetic point of view, the system is ferromagnetically homogeneous, but the e_g hole can only hop among Mn ions within certain regions. In this situation magnetic disorder cannot be responsible for the constraint of the charge. We can only consider the existence of a potential

well, which successfully traps the hole as proposed by Alonso *et al.*²³ The first contribution to this potential well could be of electrostatic origin: since we have Ca^{+2} centers surrounded by La^{+3} the hole would tend to live close to the Ca^{+2} . Also the intensity of the Jahn-Teller effect will play a role as has been suggested by Van Aken *et al.*²⁴ Alonso *et al.*²³ demonstrated that the insulating or metallic state does not depend only on the hole concentration but also on the presence of Ca^{+2} centers (holes can be produced by oxygen vacancies). Under this scheme the magnetic field is not very effective in propagating the electronic itinerancy to the whole sample. For that we must increase the Ca^{+2} concentration up to the percolation limit to reach the concentration range of the CMR compounds. We consider that our experimental result can only be explained within this frame and the theoretical model should address the ferromagnetic-insulating state within such a frame.

ACKNOWLEDGMENTS

We thank Professor A. Hernando for fruitful discussions. The Spanish authors acknowledge financial support through research Project Nos. MAT2000-1756, MAT2002-04657, and MAT2002-01221. Cz.K. and P.C.R. wish to acknowledge the support of the Engineering and Physical Sciences Research Council, United Kingdom.

*Corresponding author. FAX: 34 976 761229. Email address: algarabel@posta.unizar.es

¹C. N. R. Rao and B. Raveau, *Colossal Magnetoresistance, Charge Ordering and Related Properties of Manganese Oxides* (World Scientific, Singapore, 1998).

²J. M. D. Coey, M. Viret, and S. Von Molnar, *Adv. Phys.* **48**, 167 (1999).

³E. Dagotto, T. Hotta, and A. Moreo, *Rep. Prog. Phys.* **344**, 1 (2001).

⁴S. Jin, T. H. Tiefel, M. McCormack, R. A. Fasnacht, R. Ramesh, and L. H. Chen, *Science* **264**, 413 (1994).

⁵M. R. Ibarra, P. A. Algarabel, C. Marquina, J. Blasco, and J. García, *Phys. Rev. Lett.* **75**, 3541 (1995).

⁶J. M. De Teresa, M. R. Ibarra, P. A. Algarabel, C. Ritter, C. Marquina, J. Blasco, J. García, A. Del Moral, and Z. Arnold, *Nature (London)* **386**, 256 (1997).

⁷J. M. de Teresa, C. Ritter, M. R. Ibarra, P. A. Algarabel, J. L. García-Muñoz, J. Blasco, J. García, and C. Marquina, *Phys. Rev. B* **56**, 3317 (1997).

⁸M. R. Ibarra, Guo-meng Zhao, J. M. de Teresa, B. García-Landa, Z. Arnold, C. Marquina, P. A. Algarabel, H. Keller, and C. Ritter, *Phys. Rev. B* **57**, 7446 (1998).

⁹M. Uehara, S. Mori, C. H. Chen, and S. W. Cheong, *Nature (London)* **399**, 560 (1998).

¹⁰Cz. Kapusta, P. C. Riedi, W. Kocemba, M. R. Ibarra, and J. M. D.

Coey, *J. Appl. Phys.* **87**, 7121 (2000).

¹¹M. Hennion, F. Moussa, G. Biotteau, J. Rodriguez-Carvajal, L. Pinsard, and A. Revcolevsky, *Phys. Rev. Lett.* **81**, 1957 (1998).

¹²C. Ritter, M. R. Ibarra, J. M. de Teresa, P. A. Algarabel, C. Marquina, J. Blasco, J. García, S. Osserof, and S. W. Cheong, *Phys. Rev. B* **56**, 8902 (1997).

¹³J. E. O. Wollan and W. C. Koeler, *Phys. Rev. B* **100**, 545 (1955).

¹⁴G. Allodi, M. Cestelli, R. De Renzi, A. Carneiro, and L. Pinsard, *Phys. Rev. Lett.* **87**, 127206 (2001).

¹⁵C. Ritter (private communication).

¹⁶M. R. Ibarra and J. M. De Teresa, *J. Magn. Magn. Mater.* **177-181**, 846 (1998).

¹⁷M. L. Spano and J. J. Rhyne, *J. Appl. Phys.* **57**, 3303 (1985).

¹⁸M. M. Savosta and P. Novak, *Phys. Rev. Lett.* **87**, 137204 (2001).

¹⁹J. H. Davis and C. W. Searle, *Phys. Rev. B* **9**, 323 (1974).

²⁰Cz. Kapusta *et al.* (unpublished).

²¹G. Papavassiliou, M. Belesi, M. Fardis, and C. Dimitropoulos, *Phys. Rev. Lett.* **87**, 177204 (2001).

²²Cz. Kapusta and P. C. Riedi, *J. Magn. Magn. Mater.* **196-197**, 446 (1999).

²³J. Alonso, E. Herrero, J. M. Góñez-Calbet, M. Vallet-Regí, J. L. Martínez, J. M. Rojo, and A. Hernando, *Phys. Rev. B* **62**, 11 328 (2000).

²⁴Bas B. Van Aken, Auke Meetsma, Y. Tomioka, Y. Tokura, and Thomas T. M. Palstra, *Phys. Rev. Lett.* **90**, 066403 (2003).